



## Optimization of UV/inorganic oxidants system efficiency for photooxidative removal of an azo textile dye

Hamed Eskandarloo<sup>a</sup>, Alireza Badiei<sup>a,\*</sup>, Mohammad A. Behnajady<sup>b</sup>

<sup>a</sup>School of Chemistry, College of Science, University of Tehran, Tehran, Iran, Tel. +98 2161112614; Fax: +98 2161113301; Email: [abadiei@ut.ac.ir](mailto:abadiei@ut.ac.ir)

<sup>b</sup>Department of Chemistry, College of Science, Tabriz Branch, Islamic Azad University, Tabriz, Iran

Received 16 September 2013; Accepted 2 April 2014

### ABSTRACT

In this paper, photooxidative removal of C.I. Basic Red 46 (BR46) as a model organic pollutant was investigated in the presence of UV/inorganic oxidants system. The aim of this study was to evaluate the efficiency of hybrid oxidant system including inorganic oxidant species such as persulfate ( $S_2O_8^{2-}$ ), peroxymonosulfate ( $HSO_5^-$ ), periodate ( $IO_4^-$ ), bromate ( $BrO_3^-$ ), and chlorate ( $ClO_3^-$ ) under UV-C light irradiation. The effect of various inorganic oxidants concentration in different reaction times was predicted and optimized in the photooxidation process using response surface methodology. It was found that the concentration of inorganic oxidants significantly affected the removal rate of BR46. Modeling results showed that the predicted values of removal efficiency were found to be in good agreement with the experimental results with a correlation coefficient ( $R^2$ ) of 0.9462. Optimization results showed that maximum removal efficiency (95.51%) was achieved at the optimum oxidants concentration:  $BrO_3^-$  of  $118\text{ mg L}^{-1}$ ,  $ClO_3^-$  of  $24\text{ mg L}^{-1}$ ,  $S_2O_8^{2-}$  of  $1035\text{ mg L}^{-1}$ ,  $HSO_5^-$  of  $232\text{ mg L}^{-1}$  and  $IO_4^-$  of  $267\text{ mg L}^{-1}$  in reaction time of 23 min. Effect of oxidants concentration on the photooxidative removal of BR46 was estimated by the response surface and contour plots. Furthermore, the photooxidative removal efficiency of hybrid oxidant system mode was compared with individual processes. The obtained results clearly demonstrated that experimental design approach was one of the useful and cost-effective methods for modeling and optimizing the efficiency of UV/inorganic oxidants system. Mineralization study showed 84.4% reduction in total organic carbon value after 90 min of process.

**Keywords:** Inorganic oxidants system; Optimization; Oxidants concentration effect; Response surface methodology; C.I. Basic Red 46

### 1. Introduction

The principle sources of environmental aqueous contamination are dye pollutants, which are generally non-biodegradable and resistant to destruction by many formal methods [1,2]. Dye molecules are widely

used in paper printing, pharmaceutical, textile dyeing, cosmetic, leather, and nutrition industries. A major point of concern has been the removed dyes due to their potential toxicity and visibility in running waters [3,4]. Various physical, chemical, and biological processes are used for treatment of these textile dyes, including chemical precipitation and filtration,

\*Corresponding author.

adsorption, coagulation, electrocoagulation, biological degradation (biodegradation), ozonation, etc. [2,5].

The combination of inorganic oxidants and UV radiation provides a strong oxidant system through generation of by-products oxidants such as hydroxyl free radicals, which react with many organic compounds in water [6]. UV/inorganic oxidants extensively used as an alternative method for removal of various organic pollutants from aqueous solutions. Recently, some reports are available about the photooxidation process in the presence of UV light/inorganic oxidants such as decomposition of 2-Chlorobiphenyl by  $\text{IO}_4^-$  and  $\text{S}_2\text{O}_8^{2-}$  [7], mineralization of Calcon by  $\text{S}_2\text{O}_8^{2-}$  [8], degradation of Acid Orange 7 by  $\text{HSO}_5^-$  and  $\text{S}_2\text{O}_8^{2-}$  [9], mineralization of Ponceau S by  $\text{IO}_3^-$ ,  $\text{BrO}_3^-$ , and  $\text{S}_2\text{O}_8^{2-}$  [10], degradation of 4-fluorophenol by  $\text{BrO}_3^-$ ,  $\text{ClO}_3^-$ ,  $\text{IO}_4^-$ , and  $\text{S}_2\text{O}_8^{2-}$  [11], degradation of 4-chloro-2-methylphenol by  $\text{BrO}_3^-$ ,  $\text{ClO}_3^-$ , and  $\text{IO}_4^-$  [12], photodefluorination of pentafluorobenzoic acid by  $\text{BrO}_3^-$ ,  $\text{ClO}_3^-$ ,  $\text{IO}_4^-$ , and  $\text{S}_2\text{O}_8^{2-}$  [13], decolorization of C.I. Reactive Black 5 by  $\text{IO}_3^-$ ,  $\text{BrO}_3^-$ , and  $\text{S}_2\text{O}_8^{2-}$  [14], removal of endosulfan by  $\text{S}_2\text{O}_8^{2-}$  and  $\text{HSO}_5^-$  [15] and degradation of antipyrine by  $\text{S}_2\text{O}_8^{2-}$  [16].

Although the photooxidation efficiency of individual oxidant systems in degradation of various organic compounds has been studied in the above reports, the efficiency of hybrid oxidant system including inorganic oxidant species such as  $\text{ClO}_3^-$ ,  $\text{BrO}_3^-$ ,  $\text{H}_2\text{O}_2$ ,  $\text{S}_2\text{O}_8^{2-}$ , and  $\text{IO}_4^-$  has not yet been studied. Hybridizing of various inorganic oxidants in photooxidation process can give better results in comparison to the individual processes, due to the synergistic effect of generated different highly reactive radicals. Undergoing photolysis or thermolysis in aqueous solution,  $\text{S}_2\text{O}_8^{2-}$  decomposes to generate the reactive  $\text{SO}_4^{\cdot-}$  radicals and  $\text{HSO}_5^-$  decomposes to generate reactive radicals such as  $\text{SO}_4^{\cdot-}$  and  $\cdot\text{OH}$  [17–20]. Undergoing photolysis in aqueous solution,  $\text{IO}_4^-$  decomposes to generate the various highly reactive radical species ( $\text{O}^{\cdot-}$ ,  $\cdot\text{OH}$ ,  $\text{IO}_3^{\cdot}$  and  $\text{IO}_4^{\cdot}$ ) and non-radical intermediates ( $\text{O}_3$ ,  $\text{IO}_4^-$ , and  $\text{IO}_3^-$ ) [14]. Decomposition of  $\text{ClO}_3^-$ ,  $\text{BrO}_3^-$  under photolysis in aqueous solution, generate a number of various radical species such as  $\cdot\text{OH}$ ,  $\text{O}^{\cdot-}$ ,  $\text{O}_2^-$ , etc. [21,22]. Thus, the simultaneous use of a variety of inorganic oxidants can be associated with production of various active radical species, and thereby increase the efficiency of the photooxidation process. In this study, a hybrid system of various inorganic oxidants (such as  $\text{BrO}_3^-$ ,  $\text{ClO}_3^-$ ,  $\text{S}_2\text{O}_8^{2-}$ ,  $\text{HSO}_5^-$ , and  $\text{IO}_4^-$ ) in combined with UV-C irradiation was used for estimation of photooxidative removal of BR46 as a model organic pollutant. The effect of various inorganic oxidants concentration was predicted and optimized in the photooxidation process using RSM

technique. As the optimal concentration of each inorganic oxidant in hybrid system is needed for showing synergistic photooxidative effect, we can use response surface methodology (RSM) as a mathematical and statistical technique that is widely employed in process optimizing and modeling. RSM technique is capable of analyzing the interactions of possible influencing factors, and determining the optimum region of the factors level just using minimum number of designed experiments [23,24]. The effect of oxidants concentration on the photooxidative removal of BR46 was established by the response surface and contour plots. Furthermore, the photooxidative removal efficiency of hybrid oxidant system mode was compared with individual processes.

## 2. Materials and methods

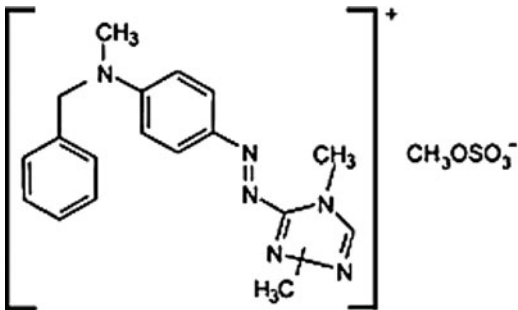
### 2.1. Reagents

Potassium bromate ( $\text{KBrO}_3$ ), potassium peroxydisulfate ( $\text{K}_2\text{S}_2\text{O}_8$ ), potassium peroxymonosulfate ( $\text{KHSO}_5$ ), potassium chlorate ( $\text{KClO}_3$ ), and potassium periodate ( $\text{KIO}_4$ ) were purchased from Merck Co. (Germany). Characteristics and chemical structure of cationic monoazo dye BR46 as a model pollutant from textile industry is given in Table 1.

### 2.2. Experimental procedure

Photooxidation processes were carried out at room temperature in a batch quartz reactor. Artificial irradiation was provided by a 15 W (UV-C) mercury lamp

Table 1  
Characteristics and chemical structure of BR46

|   |  |
|---|--|
| Other name                                    | Maxilon Red GRL-3  |
| Molecular formula                             | $\text{C}_{18}\text{H}_{24}\text{N}_6\text{O}_4\text{S}$                             |
| Molecular mass                                | $420 \text{ g mol}^{-1}$   |
| Absorption maximum ( $\lambda_{\text{max}}$ ) | 530 nm   |
| Structure                                     |  |

(Philips, Holland) emitting around 254 nm, positioned in top of the batch quartz reactor. In each run, appropriate amounts of inorganic oxidants were added in dye solution with fixed concentration of BR46 (20 mg L<sup>-1</sup>). Then the prepared solution was transferred into the continuous stirred batch quartz reactor and the lamp was switched on to initiate the irradiation. Distance between UV lamp and the solution was maintained at 5 cm, in all the measurements. At given irradiation time intervals, the samples (5 mL) were taken out, centrifuged (Sigma 2-16P), and then BR46 concentration was analyzed by UV-vis spectrophotometer (Rayleigh UV-1600) at  $\lambda_{\max} = 530$  nm. All experiments were performed in initial pH of dye solution (pH 6.1). The TOC measurements were carried out using a TOC analyzer of Shimadzu TOC-VCSH (Japan).

### 2.3. Experimental design

A central composite design (CCD) was used to propose and estimate a mathematical model of the photooxidation process behavior. Computational analysis of the experimental data was supported by the Design-Expert (version 7) software. In order to evaluate the effect of independent variables, six key factors including various inorganic oxidants concentration and reaction time were chosen and the photooxidative removal efficiency of BR46 was selected as the response. A total of 86 experiment runs were performed in this work with 10 replications at the center point. For statistical calculations, chosen variables were converted into dimensionless ones ( $x_1, x_2, x_3, x_5, x_4, x_6$ ) with the coded values at levels: -2, -1, 0, +1, +2. The experimental ranges and the levels of the chosen variables are presented in Table 2. It should be noted that the preliminary experiments were performed to determine the extreme values of the variables.

Table 2  
Experimental ranges and levels of the variables

| Variables  | Symbol<br>$x_i$ | Ranges and levels |     |     |     |       |
|--|-----------------|-------------------|-----|-----|-----|-------|
|  |                 | -2                | -1  | 0   | +1  | +2    |
| [S <sub>2</sub> O <sub>8</sub> <sup>2-</sup> ] (mg L <sup>-1</sup> ) | $x_1$           | 0                 | 200 | 550 | 900 | 1,100 |
| [HSO <sub>5</sub> <sup>-</sup> ] (mg L <sup>-1</sup> )               | $x_2$           | 0                 | 200 | 550 | 900 | 1,100 |
| [BrO <sub>3</sub> <sup>-</sup> ] (mg L <sup>-1</sup> )               | $x_3$           | 0                 | 200 | 550 | 900 | 1,100 |
| [IO <sub>4</sub> <sup>-</sup> ] (mg L <sup>-1</sup> )                | $x_4$           | 0                 | 200 | 550 | 900 | 1,100 |
| [ClO <sub>3</sub> <sup>-</sup> ] (mg L <sup>-1</sup> )               | $x_5$           | 0                 | 200 | 550 | 900 | 1,100 |
| Reaction time (min)  | $x_6$           | 7                 | 10  | 15  | 20  | 23    |

## 3. Results and discussion

In order to achieve UV/oxidants system with high photooxidative removal efficiency, oxidants concentrations in different reaction times were investigated and optimized.

### 3.1. Model results for photooxidative removal of BR46 in the presence of various inorganic oxidants

The mathematical relationship between the response and these variables can be approximated by the following second-order polynomial Eq. (1):

$$Y = b_0 + b_1x_1 + b_2x_2 + b_3x_3 + b_4x_4 + b_5x_5 + b_6x_6 + b_{12}x_1x_2 + b_{13}x_1x_3 + b_{14}x_1x_4 + b_{15}x_1x_5 + b_{16}x_1x_6 + b_{23}x_2x_3 + b_{24}x_2x_4 + b_{25}x_2x_5 + b_{26}x_2x_6 + b_{34}x_3x_4 + b_{35}x_3x_5 + b_{36}x_3x_6 + b_{45}x_4x_5 + b_{46}x_4x_6 + b_{56}x_5x_6 + b_{11}x_1^2 + b_{22}x_2^2 + b_{33}x_3^2 + b_{44}x_4^2 + b_{55}x_5^2 + b_{66}x_6^2 \quad (1)$$

where  $Y$  is a predicted response of photooxidative removal efficiency,  $b_0$  is the constant,  $b_1, b_2, b_3, b_4, b_5,$  and  $b_6$  are the regression coefficients for linear effects,  $b_{12}, b_{13}, b_{14}, b_{15}, b_{16}, b_{23}, b_{24}, b_{25}, b_{26}, b_{34}, b_{35}, b_{36}, b_{45}, b_{46},$  and  $b_{56}$  are the regression coefficients for interaction effects,  $b_{11}, b_{22}, b_{33}, b_{44}, b_{55},$  and  $b_{66}$  are the regression coefficients for squared effects and  $x_i$  is the coded experimental levels of the variables.

The details of the designed experiments along with experimental results and predicted values for photooxidative removal efficiencies of BR46 as function of oxidants concentration in different reaction times are shown in Table 3. Following the experimental design presented in Table 3, an empirical relationship between the response ( $Y$ ) and independent variables ( $x_1, x_2, x_3, x_5, x_4, x_6$ , see Table 2) was attained as shown in Eq. (2):

$$Y = 57.8 + 2.13x_1 - 2.6x_2 - 2.62x_3 - 1.16x_4 - 2.12x_5 + 6.66x_6 - 1.5x_1x_2 + 0.16x_1x_3 - 0.2x_1x_4 + 0.17x_1x_5 + 0.42x_1x_6 + 0.19x_2x_3 + 1.18x_2x_4 + 0.17x_2x_5 - 2.64x_2x_6 - 1.47x_3x_4 + 0.11x_3x_5 - 0.11x_3x_6 + 0.83x_4x_5 - 1.28x_4x_6 - 0.95x_5x_6 + 0.53x_1^2 + 3.27x_2^2 + 2.30x_3^2 + 0.89x_4^2 + 1.31x_5^2 + 1.23x_6^2 \quad (2)$$

Eq. (2) is used to predict the photooxidative removal efficiencies of organic pollutant by the UV/inorganic oxidants system with varied oxidants concentration and reaction time within the selected experimental ranges.

Table 3  
The six-factor CCD matrix with the experimental and predicted responses

| Run | Concentration of oxidants (mg L <sup>-1</sup> ) |                               |                               |                              |                               | Reaction time (min) | Removal (%)         |           |
|-----|---|-------------------------------|-------------------------------|------------------------------|-------------------------------|---------------------|---------------------|-----------|
|     | S <sub>2</sub> O <sub>8</sub> <sup>2-</sup>     | HSO <sub>5</sub> <sup>-</sup> | BrO <sub>3</sub> <sup>-</sup> | IO <sub>4</sub> <sup>-</sup> | ClO <sub>3</sub> <sup>-</sup> |                     | Experimental (±0.5) | Predicted |
| 1   | 200   | 900                           | 200                           | 200                          | 900                           | 10                  | 60.6                | 57.8      |
| 2   | 900   | 200                           | 200                           | 900                          | 200                           | 10                  | 64.4                | 67.1      |
| 3   | 900   | 900                           | 900                           | 900                          | 900                           | 10                  | 59.8                | 58.4      |
| 4   | 900   | 200                           | 200                           | 900                          | 900                           | 10                  | 63.5                | 66.1      |
| 5   | 900   | 900                           | 200                           | 900                          | 200                           | 10                  | 65.1                | 65.7      |
| 6   | 200   | 900                           | 900                           | 900                          | 900                           | 20                  | 60.4                | 60.3      |
| 7   | 200   | 900                           | 900                           | 200                          | 900                           | 10                  | 57.1                | 56.1      |
| 8   | 200   | 200                           | 200                           | 900                          | 900                           | 10                  | 60.5                | 60.1      |
| 9   | 550   | 550                           | 550                           | 550                          | 550                           | 15                  | 59                  | 57.8      |
| 10  | 200   | 200                           | 200                           | 900                          | 200                           | 20                  | 78.1                | 79        |
| 11  | 900   | 900                           | 200                           | 200                          | 900                           | 20                  | 65.4                | 68.5      |
| 12  | 550   | 550                           | 550                           | 550                          | 550                           | 15                  | 59                  | 57.8      |
| 13  | 550   | 550                           | 0                             | 550                          | 550                           | 15                  | 65.1                | 67.5      |
| 14  | 200   | 900                           | 200                           | 900                          | 200                           | 20                  | 73.7                | 73.1      |
| 15  | 110   | 550                           | 550                           | 550                          | 550                           | 15                  | 60.3                | 62.4      |
| 16  | 550   | 550                           | 550                           | 550                          | 550                           | 15                  | 57.8                | 57.8      |
| 17  | 550   | 550                           | 550                           | 550                          | 550                           | 15                  | 56.5                | 57.8      |
| 18  | 550   | 550                           | 550                           | 550                          | 550                           | 15                  | 59.9                | 57.8      |
| 19  | 550   | 550                           | 550                           | 550                          | 550                           | 23                  | 70.1                | 71.2      |
| 20  | 900   | 200                           | 200                           | 200                          | 200                           | 20                  | 89.4                | 92.4      |
| 21  | 550   | 550                           | 550                           | 110                          | 550                           | 15                  | 60.8                | 58.1      |
| 22  | 550   | 0                             | 550                           | 550                          | 550                           | 15                  | 67.6                | 69.8      |
| 23  | 200   | 200                           | 200                           | 200                          | 900                           | 20                  | 74.9                | 75.8      |
| 24  | 200   | 900                           | 200                           | 200                          | 200                           | 10                  | 61.5                | 62.1      |
| 25  | 200   | 900                           | 900                           | 200                          | 200                           | 20                  | 75.1                | 71.3      |
| 26  | 900   | 200                           | 900                           | 900                          | 900                           | 20                  | 73.6                | 73.1      |
| 27  | 550   | 550                           | 110                           | 550                          | 550                           | 15                  | 61.1                | 59.3      |
| 28  | 550   | 550                           | 550                           | 550                          | 0                             | 15                  | 64.9                | 64.3      |
| 29  | 200   | 900                           | 200                           | 900                          | 900                           | 20                  | 71.4                | 68.4      |
| 30  | 900   | 200                           | 200                           | 200                          | 900                           | 20                  | 89.2                | 84.4      |
| 31  | 900   | 200                           | 900                           | 200                          | 900                           | 20                  | 82.9                | 82.1      |
| 32  | 200   | 200                           | 900                           | 900                          | 900                           | 20                  | 61.8                | 64.7      |
| 33  | 200   | 900                           | 900                           | 900                          | 200                           | 10                  | 58.6                | 58.2      |
| 34  | 200   | 200                           | 200                           | 200                          | 200                           | 10                  | 62.1                | 62.1      |
| 35  | 200   | 900                           | 200                           | 900                          | 900                           | 10                  | 65.5                | 65.4      |
| 36  | 900   | 900                           | 900                           | 900                          | 200                           | 10                  | 59.8                | 58.2      |
| 37  | 200   | 200                           | 900                           | 200                          | 900                           | 20                  | 74.2                | 72.8      |
| 38  | 200   | 200                           | 900                           | 900                          | 200                           | 10                  | 52.7                | 52.8      |
| 39  | 900   | 900                           | 200                           | 900                          | 900                           | 20                  | 72.1                | 70.1      |
| 40  | 550   | 110                           | 550                           | 550                          | 550                           | 15                  | 63.3                | 61.7      |
| 41  | 900   | 200                           | 900                           | 900                          | 200                           | 20                  | 81                  | 77.3      |
| 42  | 200   | 900                           | 200                           | 200                          | 900                           | 20                  | 63.2                | 65.9      |
| 43  | 900   | 200                           | 900                           | 200                          | 200                           | 10                  | 67.8                | 65.9      |
| 44  | 550   | 550                           | 550                           | 550                          | 550                           | 15                  | 58                  | 57.8      |
| 45  | 900   | 900                           | 900                           | 200                          | 200                           | 20                  | 75.9                | 73.8      |
| 46  | 200   | 200                           | 200                           | 900                          | 900                           | 20                  | 72.6                | 73.6      |
| 47  | 550   | 550                           | 550                           | 550                          | 550                           | 15                  | 57.5                | 57.8      |
| 48  | 900   | 200                           | 900                           | 900                          | 900                           | 10                  | 59.3                | 58.3      |
| 49  | 200   | 200                           | 200                           | 200                          | 200                           | 20                  | 87.9                | 84.5      |
| 50  | 550   | 550                           | 550                           | 550                          | 550                           | 7                   | 50.7                | 50.3      |
| 51  | 200   | 200                           | 900                           | 200                          | 900                           | 10                  | 53.8                | 54.6      |

(Continued)

Table 3  
(Continued)

| Run | Concentration of oxidants (mg L <sup>-1</sup> ) |                               |                               |                              |                               | Reaction time (min) | Removal (%)         |           |
|-----|---|-------------------------------|-------------------------------|------------------------------|-------------------------------|---------------------|---------------------|-----------|
|     | S <sub>2</sub> O <sub>8</sub> <sup>2-</sup>     | HSO <sub>5</sub> <sup>-</sup> | BrO <sub>3</sub> <sup>-</sup> | IO <sub>4</sub> <sup>-</sup> | ClO <sub>3</sub> <sup>-</sup> |                     | Experimental (±0.5) | Predicted |
| 52  | 900   | 200                           | 200                           | 200                          | 900                           | 10                  | 66.2                | 64        |
| 53  | 900   | 900                           | 200                           | 200                          | 200                           | 20                  | 73.3                | 75.8      |
| 54  | 900   | 900                           | 900                           | 900                          | 900                           | 20                  | 59.9                | 62.6      |
| 55  | 200   | 200                           | 900                           | 200                          | 200                           | 10                  | 56.1                | 59.1      |
| 56  | 0   | 550                           | 550                           | 550                          | 550                           | 15                  | 57.2                | 55.7      |
| 57  | 900   | 200                           | 200                           | 900                          | 200                           | 20                  | 85.9                | 86        |
| 58  | 550   | 550                           | 550                           | 0                            | 550                           | 15                  | 58.4                | 61.8      |
| 59  | 900   | 900                           | 200                           | 200                          | 900                           | 10                  | 60.1                | 58.7      |
| 60  | 200   | 900                           | 900                           | 200                          | 200                           | 10                  | 58.8                | 59.8      |
| 61  | 200   | 900                           | 900                           | 900                          | 900                           | 10                  | 55                  | 57.8      |
| 62  | 900   | 200                           | 200                           | 200                          | 200                           | 10                  | 72.4                | 68.2      |
| 63  | 200   | 900                           | 200                           | 900                          | 200                           | 10                  | 64.2                | 66.4      |
| 64  | 200   | 900                           | 900                           | 900                          | 200                           | 20                  | 61.4                | 64.5      |
| 65  | 200   | 200                           | 900                           | 900                          | 900                           | 10                  | 55.9                | 51.6      |
| 66  | 200   | 200                           | 900                           | 200                          | 200                           | 20                  | 82.7                | 81.1      |
| 67  | 200   | 200                           | 200                           | 200                          | 900                           | 10                  | 55.7                | 57.1      |
| 68  | 900   | 900                           | 200                           | 900                          | 200                           | 20                  | 78.6                | 74.2      |
| 69  | 550   | 550                           | 550                           | 550                          | 110                           | 15                  | 56.4                | 57.6      |
| 70  | 900   | 900                           | 900                           | 900                          | 200                           | 20                  | 62.3                | 66.2      |
| 71  | 900   | 900                           | 900                           | 200                          | 900                           | 10                  | 56.1                | 57.5      |
| 72  | 900   | 200                           | 900                           | 900                          | 200                           | 10                  | 58.2                | 58.7      |
| 73  | 900   | 900                           | 200                           | 900                          | 900                           | 10                  | 63.6                | 65.5      |
| 74  | 550   | 550                           | 550                           | 550                          | 550                           | 15                  | 56.7                | 57.8      |
| 75  | 550   | 550                           | 550                           | 550                          | 550                           | 15                  | 58.8                | 57.8      |
| 76  | 900   | 200                           | 900                           | 200                          | 200                           | 20                  | 85.6                | 89.5      |
| 77  | 200   | 200                           | 900                           | 900                          | 200                           | 20                  | 68.7                | 69.6      |
| 78  | 900   | 900                           | 200                           | 200                          | 200                           | 10                  | 63.2                | 62.3      |
| 79  | 900   | 900                           | 900                           | 200                          | 200                           | 10                  | 59.8                | 60.6      |
| 80  | 900   | 200                           | 200                           | 900                          | 900                           | 20                  | 81                  | 81.3      |
| 81  | 900   | 900                           | 900                           | 200                          | 900                           | 20                  | 70.1                | 66.9      |
| 82  | 200   | 900                           | 200                           | 200                          | 200                           | 20                  | 72.7                | 74        |
| 83  | 200   | 900                           | 900                           | 200                          | 900                           | 20                  | 63.1                | 63.7      |
| 84  | 900   | 200                           | 900                           | 200                          | 900                           | 10                  | 59.1                | 62.1      |
| 85  | 550   | 550                           | 550                           | 550                          | 550                           | 15                  | 56.9                | 57.8      |
| 86  | 200   | 200                           | 200                           | 900                          | 200                           | 10                  | 63                  | 61.6      |

The Pareto analysis is a method that gives more significant information to interpret the results. This analysis calculates the percentage effect of each factor on the response, according to Eq. (3) [25,26]:

$$P_i = \left( \frac{b_i^2}{\sum b_i^2} \right) \times 100 \quad (i \neq 0) \quad (3)$$

The Pareto graph is displayed in Fig. 1. As can be observed, among the variables, reaction time ( $b_6$ , 42.24%) and squared effect of [HSO<sub>5</sub><sup>-</sup>] ( $b_{22}$ , 10.18%) have the largest effect on photooxidative removal efficiency of BR46.

Using resulted second-order polynomial equation (Eq. (2)), the predicted values of photooxidative removal of BR46 are plotted versus corresponding experimental results in Fig. 2. Results confirm that the predicted photooxidative removal efficiencies for BR46 as function of oxidants concentration and reaction time from the model are in good agreement with the experimental results.

Analysis of variance (ANOVA) of the quadratic response surface model is a mean to test the significance and adequacy of the model [27]. Table 4 shows the ANOVA results for quadratic response surface model. According to the ANOVA results, the regression model presents a high correlation coefficients

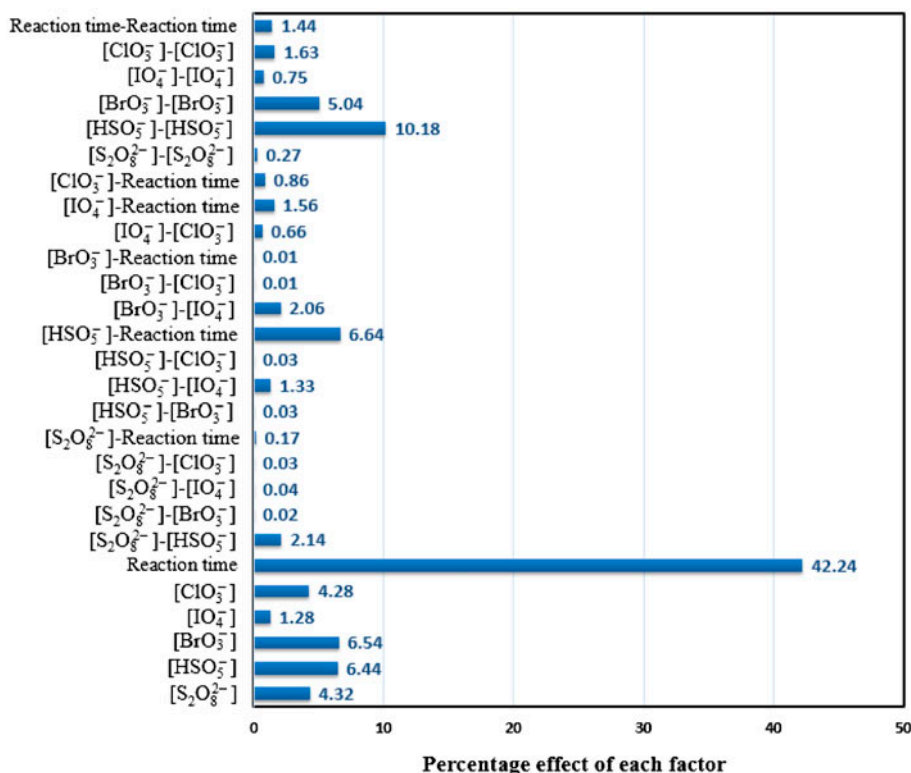


Fig. 1. Pareto graph analysis ( $[BR46]_0 = 20 \text{ mg L}^{-1}$ , initial solution pH 6.1, and  $T = 25 \pm 1^\circ\text{C}$ ).

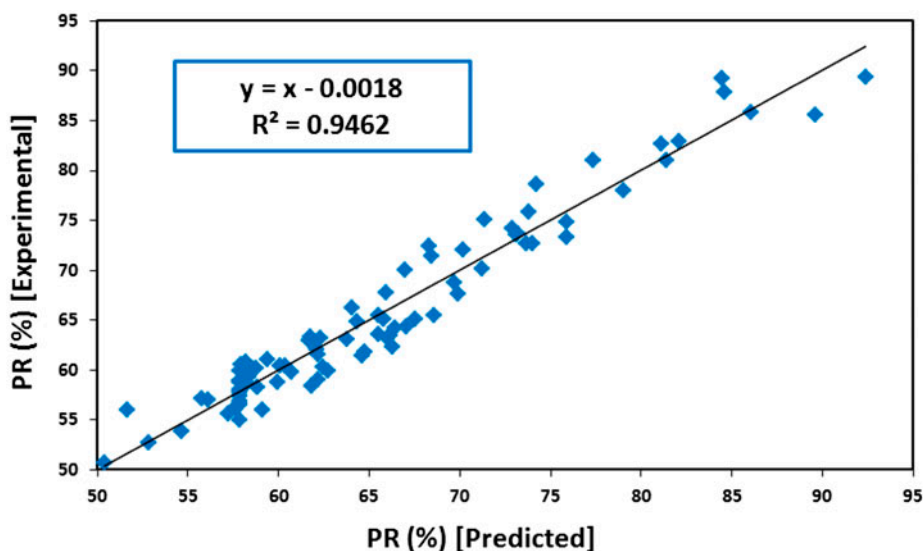


Fig. 2. Comparison between predicted and experimental removal (%) values ( $[BR46]_0 = 20 \text{ mg L}^{-1}$ , initial solution pH 6.1, and  $T = 25 \pm 1^\circ\text{C}$ ).

( $R^2 = 0.9462$ ) for the photooxidative removal of BR46. The value of  $R^2$  implies a satisfactory representation of photooxidation process by the model. Adjusted  $R^2$

is also used to measure the goodness-of-fit between model and experimental data. In the study, the effect of independent variables, adjusted  $R^2$  values (0.9212),

Table 4  
ANOVA results of the response surface quadratic model for the photooxidative removal of BR46

| Source of variations | Sum of squares | Degree of freedom | Mean square | F-value | p-value |
|----------------------|----------------|-------------------|-------------|---------|---------|
| Regression           | 6,805.52       | 27                | 252.06      | 37.82   | <0.0001 |
| Residual             | 3,86.57        | 58                | 6.66        |         |         |
| Total                | 7,192.09       | 85                |             |         |         |

Note:  $R^2=0.9463$ , adjusted  $R^2=0.9212$ .

was very close to the corresponding  $R^2$  values. The  $F$  value is the ratio between the mean square of the model and the residual error, and indicates the significance of each controlled factor on the tested model [28]. The  $F$  values for the model is 37.82 and the corresponding  $p$  value is <0.0001. These results indicated that the model was statistically significant and there is only a 0.01% chance that the “model  $F$  value” could occur due to noise.

### 3.2. Influence of various inorganic oxidants concentration on photooxidation process as response surface and contour plots

Response surface plots provide a method to predict the photooxidative removal efficiency for different values of the tested variables. In addition, the contour plots help in identification of the type of interactions between oxidants concentration and reaction time. The response surface and contour plots for various inorganic oxidants concentration, while concentration of four oxidant kept at their respective zero level and the concentration of one oxidant varying within the experimental ranges with reaction time, are obtained using the statistical software to evaluate the interactive relationships between the selected factors and photooxidative removal of BR46.

#### 3.2.1. Influence of $\text{ClO}_3^-$ concentration

The chlorate is an inorganic salt that functions as an oxidizing agent particularly in the presence of strong acid, which is used for various medical, veterinary, and miscellaneous purposes. Chlorate anion is unstable in water and decomposes to form hypochlorite and oxygen and reacts readily with organic materials [21]. The decomposition of  $\text{ClO}_3^-$  under UV irradiation is summarized in the following reactions (Eqs. (4)–(9)):

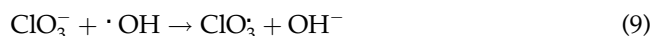


Fig. 3 shows the effect of  $\text{ClO}_3^-$  concentration (in the range of 0–1,100  $\text{mg L}^{-1}$ ) and reaction time on photooxidative removal of BR46, while concentration of other oxidants kept at its respective zero level (550  $\text{mg L}^{-1}$ ). As can be seen from the response surface and contour plots, removal rate of BR46 decreased with increasing the  $\text{ClO}_3^-$  concentration. An appropriate concentration of  $\text{ClO}_3^-$  oxidant is necessary to reaching high photooxidative removal rate of BR46. The contour plots (Fig. 3) indicate that the highest photooxidative removal rate ( $\geq 80\%$ ) is achieved when  $\text{ClO}_3^-$  concentration is relatively less than 200  $\text{mg L}^{-1}$ .

#### 3.2.2. Influence of $\text{BrO}_3^-$ concentration

Bromate is an inorganic disinfection in the mineralization process with an oxidation potential of 1.4 V in acidic medium [10]. Bromate under photolysis in aqueous solution decompose to generate a number of various radical species,  $\text{BrO}_3^\bullet$ ,  $\cdot\text{OH}$ ,  $\text{O}^-$ ,  $\text{O}_2^-$ , etc. which the formation of these reactive species is responsible for the photooxidative activity of bromate. Zuo and Katsumura suggested Eqs. (10)–(15) as photolytic decomposition mechanism of  $\text{BrO}_3^-$  under UV irradiation [22].



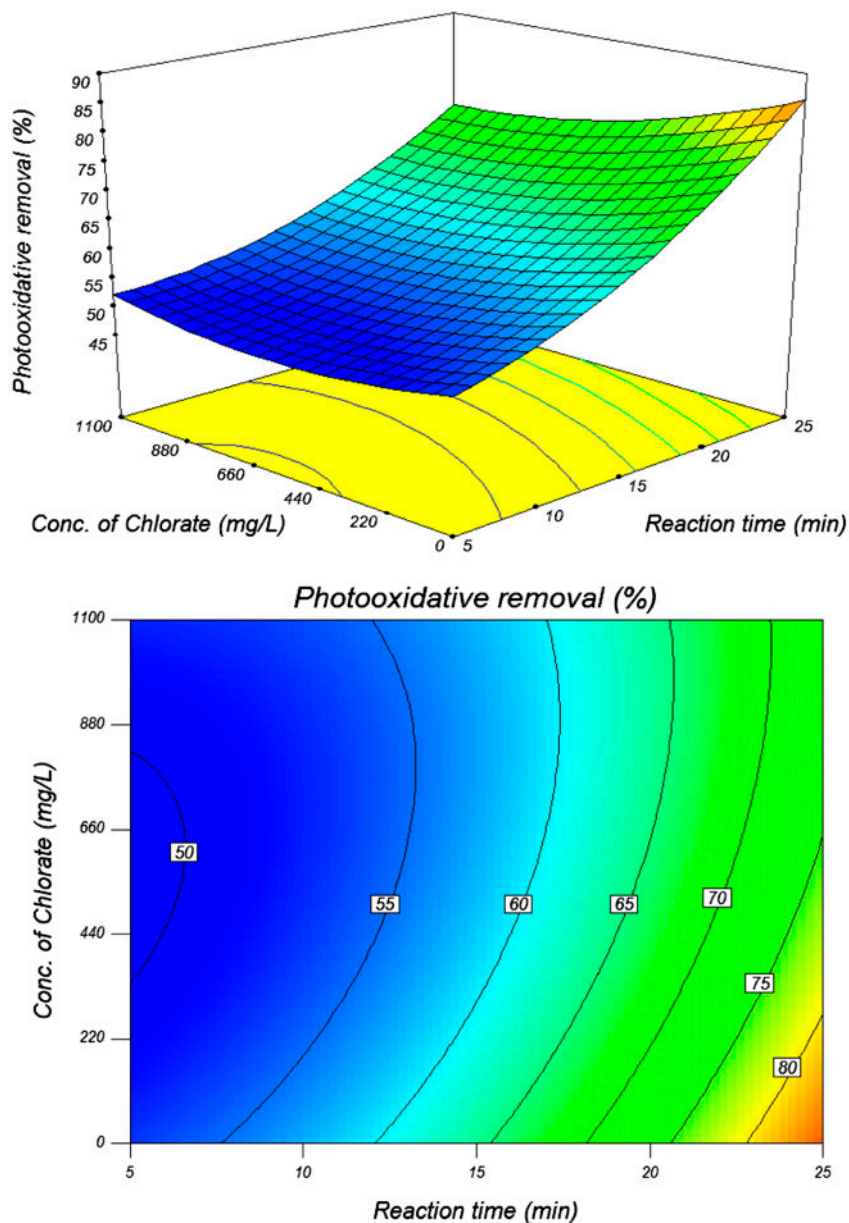
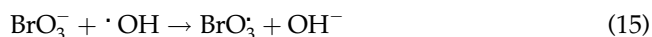


Fig. 3. The response surface and contour plots of photooxidative removal of BR46 as the function of chlorate concentration and reaction time ( $[BR46]_0 = 20 \text{ mg L}^{-1}$ , initial solution pH 6.1, and  $T = 25 \pm 1^\circ \text{C}$ ).



In order to find out the effect of  $\text{BrO}_3^-$  concentration on photooxidative removal of BR46, the experiments were carried out with  $\text{BrO}_3^-$  concentration varying in the range of 0–1,100  $\text{mg L}^{-1}$  while concentration of other oxidants kept at their respective zero level

(550  $\text{mg L}^{-1}$ ). Fig. 4 shows the effect of the  $\text{BrO}_3^-$  concentration on the photooxidative removal of BR46 established by the response surface and contour plots. As can be seen from this figure, the increase in the  $\text{BrO}_3^-$  concentration slightly declines the removal rate of BR46 in aqueous solution. This slightly decreased photooxidative removal of BR46 with  $\text{BrO}_3^-$  dose addition maybe a consequence of  $\cdot\text{OH}$  radicals scavenging by excessive  $\text{BrO}_3^-$  ions, according to Eq. (15). For all concentrations of  $\text{BrO}_3^-$  oxidant, highest removal was

obtained after reaction time of 23 min. The contour plots (Fig. 4) show that the optimum  $\text{BrO}_3^-$  concentration for highest photooxidative removal of BR46 ( $\geq 80\%$ ) is achieved when  $\text{BrO}_3^-$  concentration is less than  $220 \text{ mg L}^{-1}$  and reaction time is maintained at its maximum values.

### 3.2.3. Influence of $\text{HSO}_5^-$ concentration

Peroxymonosulfate is an inexpensive and effective acidic oxidant for the transformation of a wide range of organic compounds. Undergoing photolysis or thermolysis in aqueous solution,  $\text{HSO}_5^-$  decomposes to generate reactive radicals such as  $\text{SO}_4^{\cdot-}$  and  $\cdot\text{OH}$  [17,18]. Moreover, unlike the symmetrical structure of  $\text{S}_2\text{O}_8^{2-}$ ,  $\text{HSO}_5^-$  is an unsymmetrical peroxide, which is considered to be more easily activated than  $\text{S}_2\text{O}_8^{2-}$  [29,30]. Guan et al. confirmed the formation of  $\text{SO}_4^{\cdot-}$  and  $\cdot\text{OH}$  in the UV/ $\text{HSO}_5^-$  system and found that the rate of  $\text{HSO}_5^-$  photolysis into  $\text{SO}_4^{\cdot-}$  and  $\cdot\text{OH}$  increased with the value of pH at the range of 8–10 [31]. The photolytic decomposition of  $\text{HSO}_5^-$  under UV irradiation is summarized in the following reactions (Eqs. (16)–(21)) [17,18]:

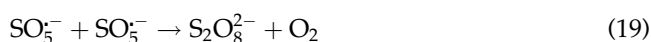
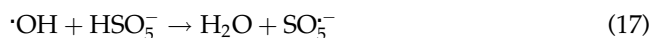


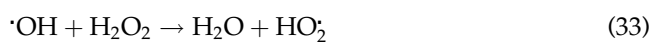
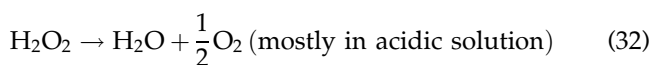
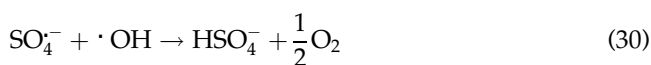
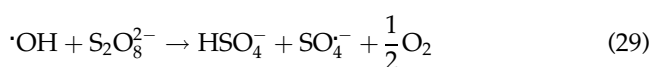
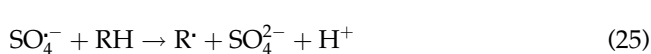
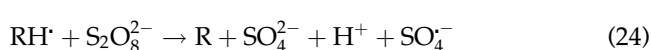
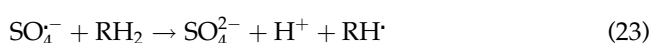
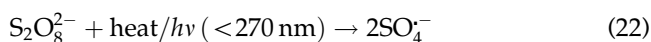
Fig. 5 shows the effect of the  $\text{HSO}_5^-$  concentration and reaction time on the photooxidative removal of BR46 while concentration of other oxidants was kept at their respective zero level ( $550 \text{ mg L}^{-1}$ ). In order to find out the effect of  $\text{HSO}_5^-$  concentration on photooxidation process, the experiments were carried out with  $\text{HSO}_5^-$  concentration varying in the range of 0–1,100  $\text{mg L}^{-1}$ . As can be seen from the response surface and contour plots, photooxidative removal of BR46 decreased with increasing the concentration of  $\text{HSO}_5^-$ . Possibly, the employing of higher concentration of  $\text{HSO}_5^-$  ions from desired concentration leads to generate the excessive  $\cdot\text{OH}$  radicals, which recombination of excessive  $\cdot\text{OH}$  radicals to forms less reactive  $\text{H}_2\text{O}_2$  molecules and thus decreases the rate of BR46 removal. It is obvious in contour plots (Fig. 5) that the highest removal of

BR46 ( $\geq 90\%$ ) is achieved when  $\text{HSO}_5^-$  concentration is relatively less than  $200 \text{ mg L}^{-1}$  and reaction time is maintained at its maximum values.

### 3.2.4. Influence of $\text{S}_2\text{O}_8^{2-}$ concentration

Peroxydisulfate is a thermodynamically strong oxidizing agent (with redox potential of 2.05 V) that has been used as a sacrificial reagent and alternative oxidant in the chemical oxidation of organic contaminants [19,32]. Reactions of peroxydisulfate with many organic compounds is slow at normal temperature; however, undergoing photolysis or thermolysis in aqueous solution,  $\text{S}_2\text{O}_8^{2-}$  decomposes to generate the free sulfate ( $\text{SO}_4^{\cdot-}$ ) oxidant [17,18]. This radical as a very strong oxidizing agent (with redox potential of 2.6 V) can accelerate the reaction through producing a rapid attack to any oxidizable agent [33].

Both sulfate and hydroxyl radicals are possibly responsible for the degradation and mineralization of organic compounds in the contaminated water, but the  $\text{SO}_4^{\cdot-}$  radical is more efficient in destruction of organic molecules than  $\text{HO}\cdot$  radical [34]. The decomposition of  $\text{S}_2\text{O}_8^{2-}$  under UV irradiation is summarized in the following reactions (Eqs. (22)–(34)) [19,20,32,35]:





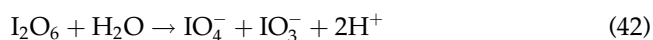
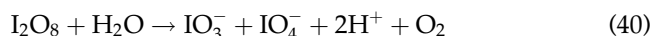
where  $R$  is an organic reagent.

$\text{SO}_4^{\cdot-}$  and  $\cdot\text{OH}$  radicals react with organic molecules mainly by three different ways: hydrogen abstracting from saturated carbon, hydrogen addition to unsaturated or aromatic hydrocarbons, and electron removing from anions [36].

In order to find out the effect of  $\text{S}_2\text{O}_8^{2-}$  concentration on photooxidative removal of BR46, the experiments were carried out with  $\text{S}_2\text{O}_8^{2-}$  concentration varying in the range of 0–1,100 mg L<sup>-1</sup> while concentration of other oxidants kept at its respective zero level (550 mg L<sup>-1</sup>). Fig. 6 shows the effect of the  $\text{S}_2\text{O}_8^{2-}$  concentration and reaction time on the photooxidative removal of BR46. It could be seen from this figure that the increase in the  $\text{S}_2\text{O}_8^{2-}$  concentration from 0 to 1,100 mg L<sup>-1</sup> slightly improves the removal of BR46. This improved photooxidative removal of BR46 can be in consequence of more  $\text{SO}_4^{\cdot-}$  and  $\cdot\text{OH}$  radicals generation, according to Eqs. (22) and (27). However, some studies have reported that the employing of higher concentration of  $\text{S}_2\text{O}_8^{2-}$  oxidant leads to generate the excessive  $\cdot\text{OH}$  radicals. Therefore, recombination of excessive  $\cdot\text{OH}$  radicals to form less reactive  $\text{H}_2\text{O}_2$  molecules (Eq. (31)) [32,35,37]. On the other hand, photooxidative removal of BR46 increased with increasing reaction time. For all concentrations of  $\text{S}_2\text{O}_8^{2-}$  oxidant, highest removal was obtained after reaction time of 23 min. It is obvious in Fig. 6 that oxidant concentration effect on BR46 removal is less significant relative to the reaction time. The contour plots (Fig. 6) show that the optimum  $\text{S}_2\text{O}_8^{2-}$  concentration for highest photooxidative removal of BR46 ( $\geq 80\%$ ) is achieved when  $\text{S}_2\text{O}_8^{2-}$  concentration is relatively higher than 900 mg L<sup>-1</sup> and reaction time is maintained at its maximum values.

### 3.2.5. Influence of $\text{IO}_4^-$ concentration

Periodate was described as an inorganic oxidant which can rapidly oxidize a wide range of organic compounds, that most of the organic compounds have the amine, imine, or glycol group [7,38]. Periodate under photolysis in aqueous solution decomposes to generate a number of highly reactive radicals and non-radical intermediates. Weavers et al. investigated the photolytic decomposition mechanism of  $\text{IO}_4^-$  under UV irradiation (254 nm), as given by Eqs. (35)–(42) [39–41].



The formation of various highly reactive radical species ( $\text{O}^{\cdot-}$ ,  $\cdot\text{OH}$ ,  $\text{IO}_3^{\cdot}$ , and  $\text{IO}_4^{\cdot}$ ) and non-radical intermediates ( $\text{O}_3$ ,  $\text{IO}_4^-$ , and  $\text{IO}_3^-$ ) is responsible for the high activity of UV/ $\text{IO}_4^-$  [14]. These reactive radical intermediates generated from photolysis of  $\text{IO}_4^-$  in aqueous solution, attack the azo groups (N=N) of the BR46 molecules and cause oxidative cleavage by free radical pathways.

Fig. 7 shows the effect of  $\text{IO}_4^-$  concentration (in the range of 0 to 1,100 mg L<sup>-1</sup>) and reaction time on photooxidative removal of BR46, while concentration of other oxidants kept at their respective zero level (550 mg L<sup>-1</sup>). As can be understood from the response surface and contour plots, removal rate of BR46 slightly decreased with increasing the  $\text{IO}_4^-$  concentration. An appropriate concentration of  $\text{IO}_4^-$  oxidant is necessary for reaching to high photooxidative removal rate. The contour plots (Fig. 7) indicate that the highest photooxidative removal of BR46 ( $\geq 80\%$ ) is achieved when  $\text{IO}_4^-$  concentration is relatively less than 220 mg L<sup>-1</sup>. Some studies have reported that increasing the concentration of periodate in aqueous solution leads to an increase in the number of radicals formed and so higher removal rate of the organic compound was achieved in a short time. However, the presence of high concentration of  $\text{IO}_4^-$  oxidant in solution may scavenge the hydroxyl radicals (Eq. (37)) and decrease the efficiency of photooxidation process in BR46 removal.

From results of Figs. 3–5 and 7, we conclude that in the case of  $\text{ClO}_3^-$ ,  $\text{HSO}_5^-$ ,  $\text{BrO}_3^-$ , and  $\text{IO}_4^-$  oxidant agents, the optimal concentration is relatively less than 200 mg L<sup>-1</sup>, while for  $\text{S}_2\text{O}_8^{2-}$  oxidant agent the optimal concentration is relatively higher than 900 mg L<sup>-1</sup>.

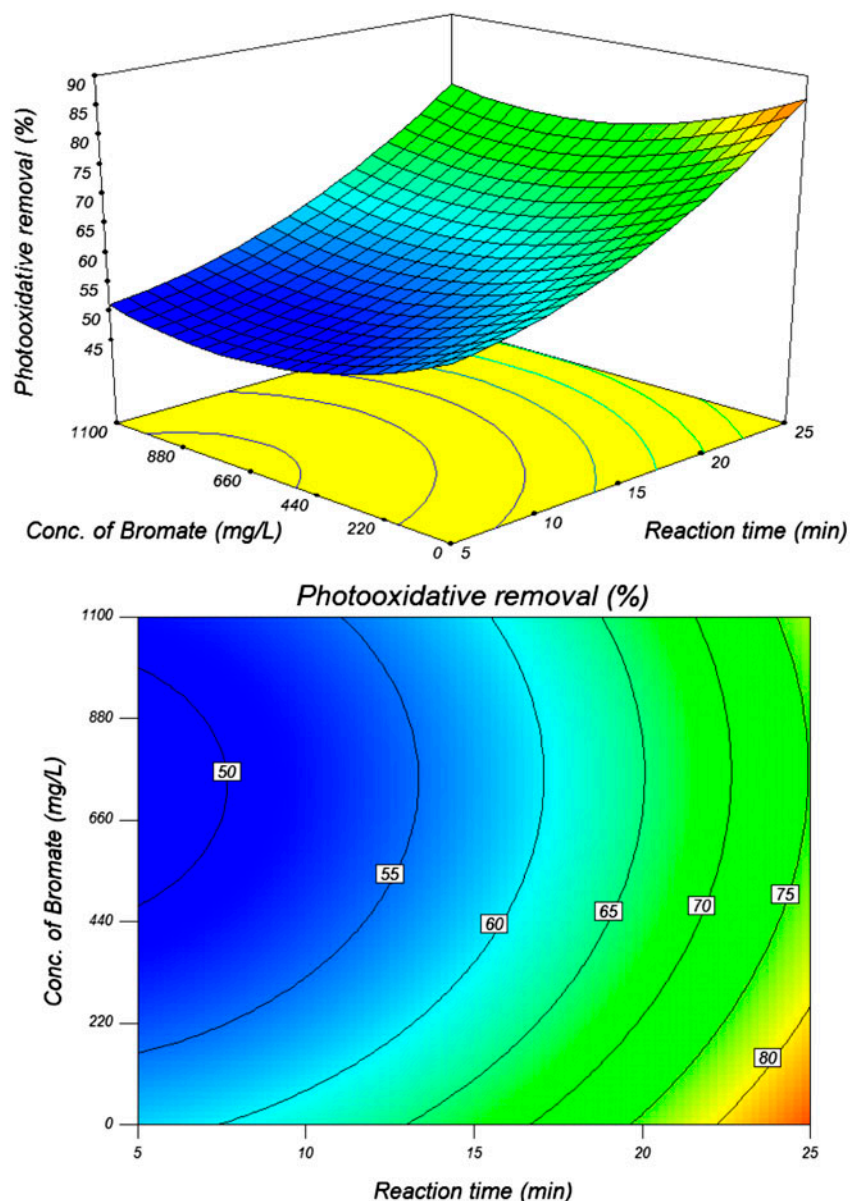


Fig. 4. The response surface and contour plots of photooxidative removal of BR46 as the function of bromate concentration and reaction time ( $[BR46]_0 = 20 \text{ mg L}^{-1}$ , initial solution pH 6.1, and  $T = 25 \pm 1^\circ\text{C}$ ).

### 3.3. Determination of optimal conditions for photooxidative removal of BR46

The main objective in terms of photooxidative removal efficiency was defined as “maximize” to achieve optimum values of various inorganic oxidants concentration. Design Expert as a response optimizer software was used for the optimization of oxidants concentration in the selected range ( $0\text{--}1,100 \text{ mg L}^{-1}$ ). The optimal concentration of the inorganic oxidants for the maximum photooxidative removal efficiency with predicted and observed PR (%) is shown in

Table 5. The optimum values of oxidants concentration are  $118$ ,  $24$ ,  $1,035$ ,  $232$ , and  $267 \text{ mg L}^{-1}$  for  $\text{BrO}_3^-$ ,  $\text{ClO}_3^-$ ,  $\text{S}_2\text{O}_8^{2-}$ ,  $\text{HSO}_5^-$ , and  $\text{IO}_4^-$ , respectively, in 23-min reaction time. As consequent, experimental design strategy can be a successful investigation to determine the optimum values of inorganic oxidants concentration and can be an adequate modeling to predict photooxidative removal efficiency.

Furthermore, the photooxidative removal of BR46 in aqueous solution by hybrid oxidant system mode was compared with individual processes (UV/ $\text{BrO}_3^-$ ,

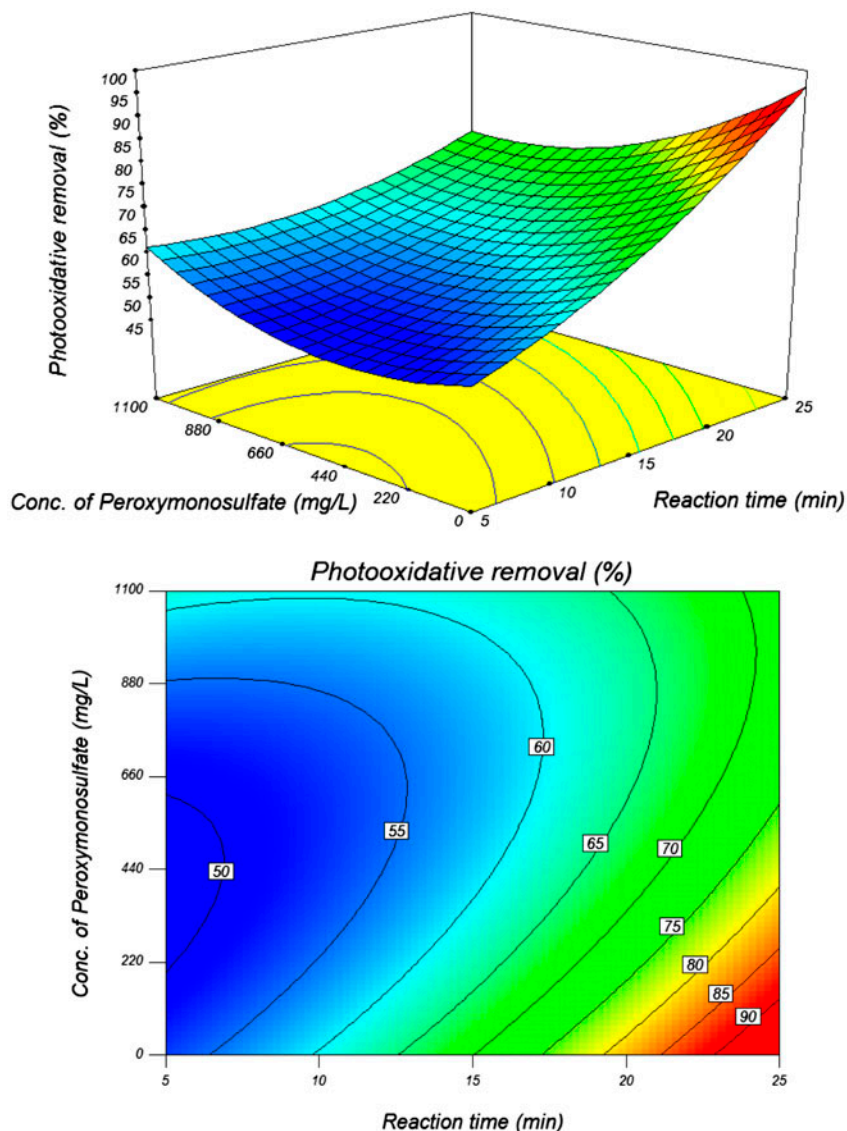


Fig. 5. The response surface and contour plots of photooxidative removal of BR46 as the function of peroxymonosulfate concentration and reaction time ( $[BR46]_0 = 20 \text{ mg L}^{-1}$ , initial solution pH 6.1, and  $T = 25 \pm 1^\circ \text{C}$ ).

UV/ $\text{ClO}_3^-$ , UV/ $\text{S}_2\text{O}_8^{2-}$ , UV/ $\text{HSO}_5^-$  and UV/ $\text{IO}_4^-$ ) in optimized conditions. The experimental results are presented in Fig. 8. A photooxidative removal of 95.51% was obtained in UV/hybrid oxidant system mode versus 1.42, 8.31, 11.75, 36.54, 65.98, and 73.14% for individual direct photolysis, UV/ $\text{ClO}_3^-$ , UV/ $\text{BrO}_3^-$ , UV/ $\text{HSO}_5^-$ , UV/ $\text{S}_2\text{O}_8^{2-}$ , and UV/ $\text{IO}_4^-$  after 23 min of reaction time. Therefore, the synergistic effect was achieved by hybridizing of inorganic oxidant system in photooxidation process than individual processes. Selvam et al. explained difference between removal efficiency of 4-fluorophenol by some oxidants (such as  $\text{ClO}_3^-$ ,  $\text{BrO}_3^-$ ,  $\text{H}_2\text{O}_2$ ,  $\text{S}_2\text{O}_8^{2-}$

and  $\text{IO}_4^-$ ) through UV absorption spectra of each oxidants. The UV absorption of these oxidants was found to be in the order of  $\text{KIO}_4 > (\text{NH}_4)_2\text{S}_2\text{O}_8 > \text{H}_2\text{O}_2 > \text{KBrO}_3 > \text{KClO}_3$ . They reported that the higher removal efficiency of  $\text{IO}_4^-$  is due to its high absorption of UV light, while  $\text{ClO}_3^-$  with least removal efficiency has no UV absorption [11]. The same results was found by Irmak et al. in photooxidative removal of 4-chloro-2-methylphenol, they reported that the oxidant with higher UV absorption is more effective on degradation of organic compounds due to high absorption of UV light leads to formation of reactive radical species [12].

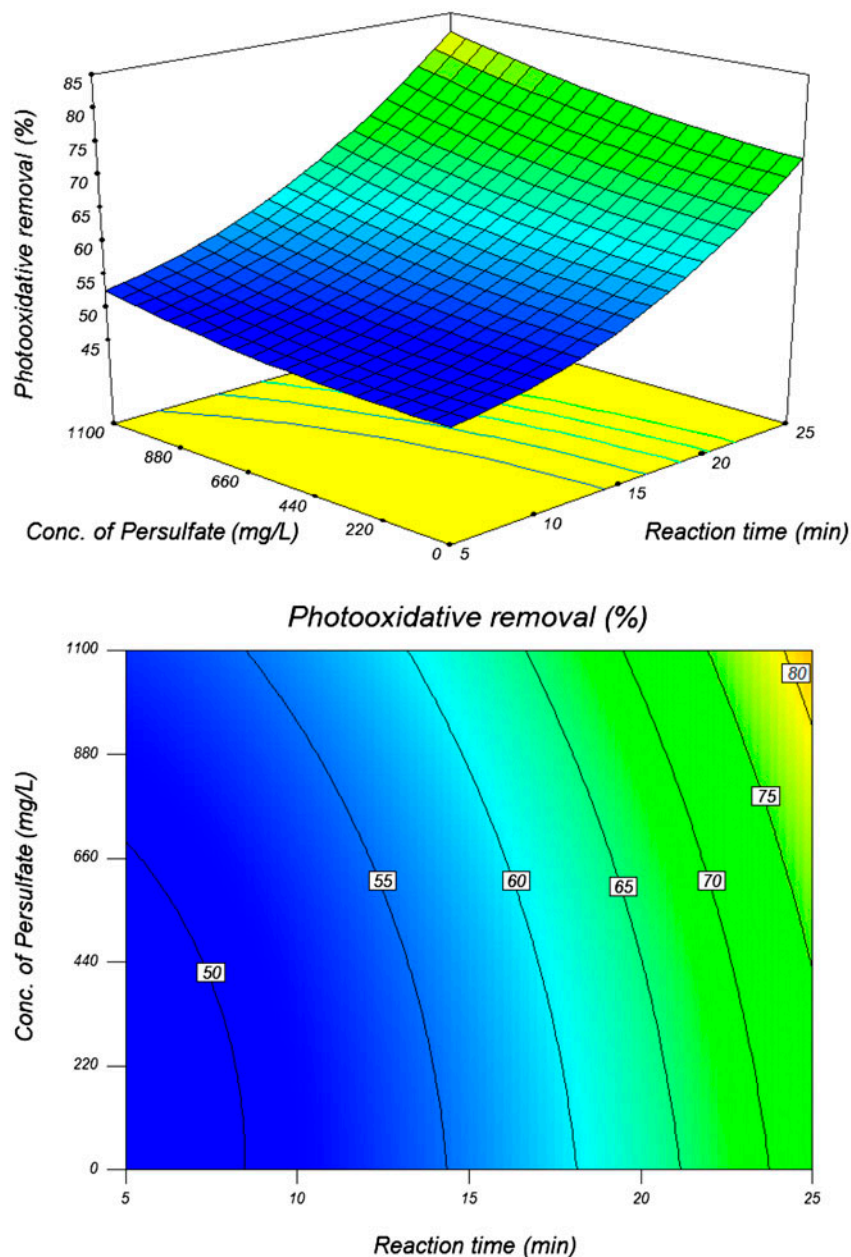


Fig. 6. The response surface and contour plots of photooxidative removal of BR46 as the function of persulfate concentration and reaction time ( $[BR46]_0 = 20 \text{ mg L}^{-1}$ , initial solution pH 6.1, and  $T = 25 \pm 1^\circ\text{C}$ ).

### 3.4. Mineralization of BR46

Mineralization of BR46 by hybrid oxidant system under optimized conditions was studied through disappearance of UV-vis peaks and TOC loss. The absorbance of BR46 at  $\lambda = 254 \text{ nm}$  is responsible for aromatic ring content attached to the  $-\text{N}=\text{N}-$  group in the BR46 molecular structure [42,43]. The disappearance of BR46 aromatic ring content in the aqueous solution was measured using the band intensity at 254 nm after

23 min irradiation time. The results showed 74.1% reduction at 254 nm absorbance intensity, which indicates degradation and mineralization of BR46 aromatic ring. Also, to study the mineralization of BR46 by hybrid oxidant system, the TOC measurements were carried out at the initial BR46 concentration of  $20 \text{ mg L}^{-1}$  (Fig. 9). The results of TOC showed 84.4% reduction in the TOC value after 90 min of irradiation time.

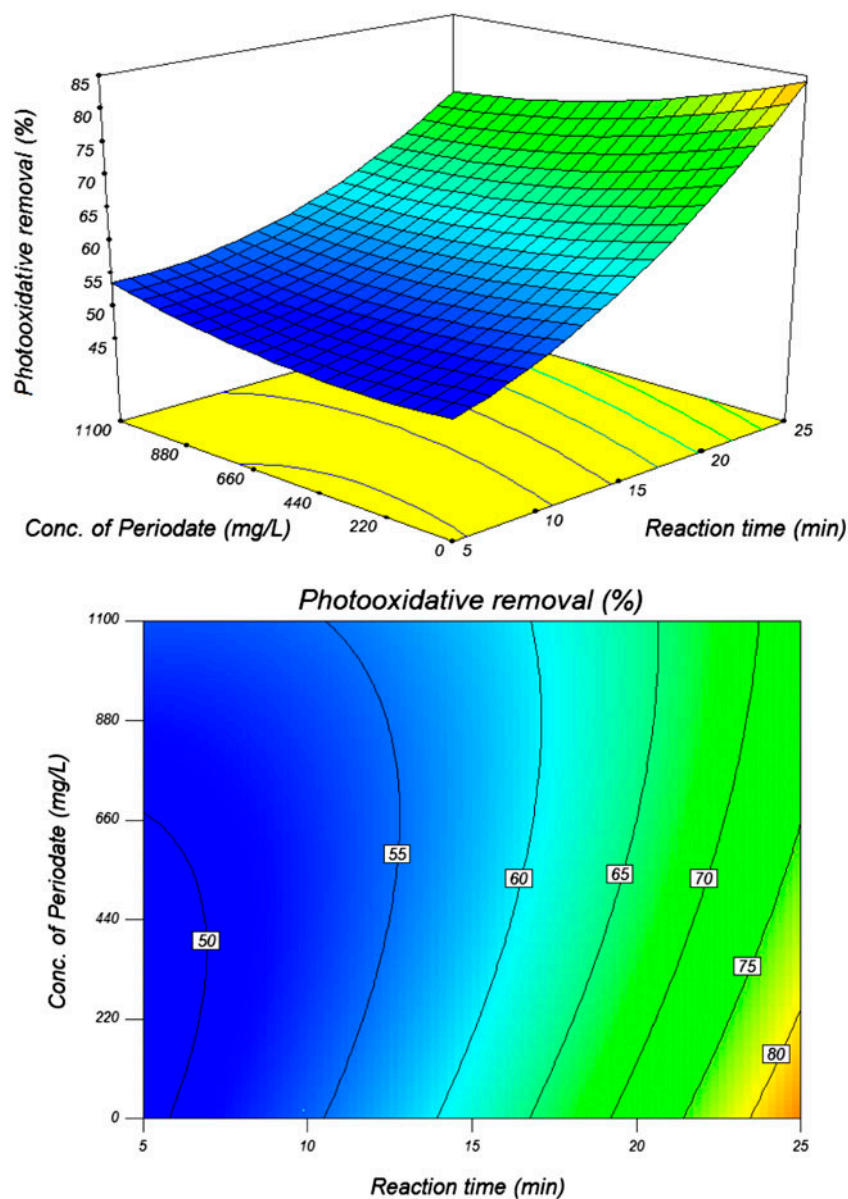


Fig. 7. The response surface and contour plots of photooxidative removal of BR46 as the function of periodate concentration and reaction time ( $[BR46]_0 = 20 \text{ mg L}^{-1}$ , initial solution pH 6.1, and  $T = 25 \pm 1 \text{ }^\circ\text{C}$ ).

Table 5

Optimum values of various inorganic oxidants concentration and reaction time for maximum photooxidative removal of BR46

| Concentration of oxidants ( $\text{mg L}^{-1}$ ) |                  |                  |                 |                  | Reaction time (min) | PR (%)    |          |
|--|------------------|------------------|-----------------|------------------|---------------------|-----------|----------|
| $\text{S}_2\text{O}_8^{2-}$                      | $\text{HSO}_5^-$ | $\text{BrO}_3^-$ | $\text{IO}_4^-$ | $\text{ClO}_3^-$ |                     | Predicted | Observed |
| 1,035  | 232              | 118              | 267             | 24               | 23                  | 96.19     | 95.51    |

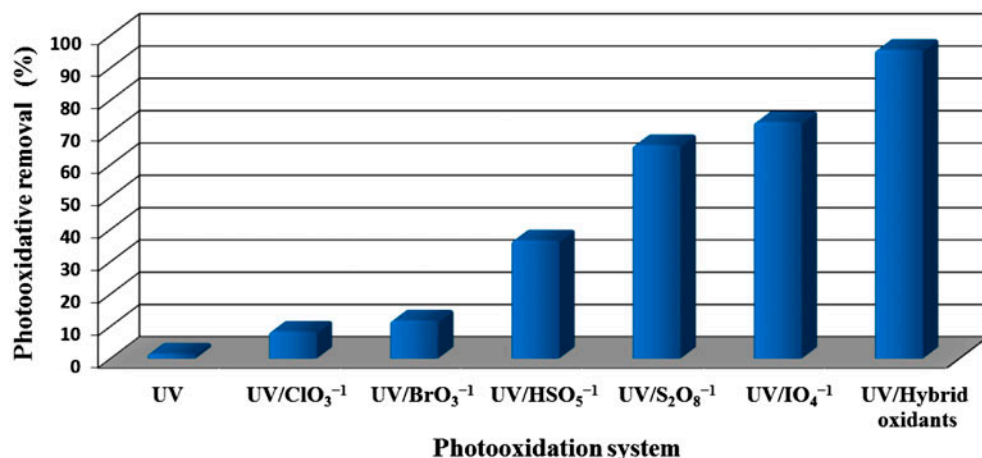


Fig. 8. Comparison of the photooxidative removal efficiency of hybrid oxidant system with individuals in optimized conditions ( $[BR46]_0 = 20 \text{ mg L}^{-1}$ , initial solution pH 6.1, and  $T = 25 \pm 1^\circ \text{C}$ ).

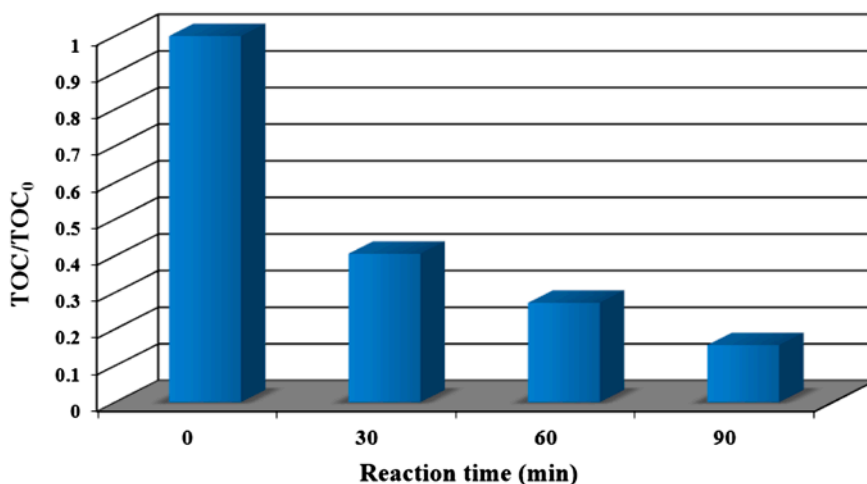


Fig. 9. TOC decay during photooxidative removal of BR46 by hybrid oxidant system ( $[BR46]_0 = 20 \text{ mg L}^{-1}$ , initial solution pH 6.1, and  $T = 25 \pm 1^\circ \text{C}$ ).

#### 4. Conclusions

In this study, RSM employed to optimize and predict the individual and interaction effects of the various inorganic oxidants in the photooxidation process. The results showed that the predicted values of removal efficiency were found to be in good consistency with experimental results with a correlation coefficient ( $R^2$ ) of 0.9462. Optimization results showed that maximum photooxidative removal efficiency (95.51%) was achieved at the optimum oxidants concentration: BrO<sub>3</sub><sup>-</sup> of 118 mg L<sup>-1</sup>, ClO<sub>3</sub><sup>-</sup> of 24 mg L<sup>-1</sup>, S<sub>2</sub>O<sub>8</sub><sup>2-</sup> of 1,035 mg L<sup>-1</sup>, HO<sub>4</sub><sup>-</sup> of 232 mg L<sup>-1</sup>, and IO<sub>4</sub><sup>-</sup> of

267 mg L<sup>-1</sup> in reaction time of 23 min. A photooxidative removal of 95.51% was obtained in UV/hybrid oxidant system mode versus 1.42, 8.31, 11.75, 36.54, 65.98, and 73.14% for individual direct photolysis, UV/ClO<sub>3</sub><sup>-</sup>, UV/BrO<sub>3</sub><sup>-</sup>, UV/HSO<sub>5</sub><sup>-</sup>, UV/S<sub>2</sub>O<sub>8</sub><sup>2-</sup>, and UV/IO<sub>4</sub><sup>-</sup> after 23 min of reaction time. Our results clearly demonstrated that RSM technique with a CCD was one of the useful and cost-effective methods in modeling and optimizing the efficiency of UV/inorganic oxidants system. TOC measurement showed that the hybrid oxidant system could mineralize the BR46 solution.

## Acknowledgment

The authors thank University of Tehran for the supporting this work.

## References

- [1] G. Chantal, H. Lachheb, A. Houas, M. Ksibi, E. Elaloui, J.M. Herrmann, Influence of chemical structure of dyes, of pH and of inorganic salts on their photocatalytic degradation by TiO<sub>2</sub> comparison of the efficiency of powder and supported TiO<sub>2</sub>, *J. Photochem. Photobiol., A* 158 (2003) 27–36.
- [2] N. Daneshvar, M.A. Behnajady, M. Khayyat Ali Mohammadi, M.S. Seyed Dorraji, UV/H<sub>2</sub>O<sub>2</sub> treatment of Rhodamine B in aqueous solution: Influence of operational parameters and kinetic modeling, *Desalination* 230 (2008) 16–26.
- [3] M.A. Behnajady, H. Eskandarloo, N. Modirshahla, M. Shokri, Influence of the chemical structure of organic pollutants on photocatalytic activity of TiO<sub>2</sub> nanoparticles: Kinetic analysis and evaluation of electrical energy per order (E<sub>EO</sub>), *Dig. J. Nanomater. Biostruct.* 6 (2011) 1887–1895.
- [4] S. Ren, J. Guo, G. Zeng, G. Sun, Decolorization of triphenylmethane, azo, and anthraquinone dyes by a newly isolated *Aeromonas hydrophila* strain, *Appl. Microbiol. Biotechnol.* 72 (2006) 1316–1321.
- [5] S.G. Schrank, J.N.R. Santos, D.S. Souza, E.E.S. Souza, Decolourisation effects of Vat Green 01 textile dye and textile wastewater using H<sub>2</sub>O<sub>2</sub>/UV process, *J. Photochem. Photobiol., A* 186 (2007) 125–129.
- [6] R. Hazime, Q.H. Nguyen, C. Ferronato, A. Salvador, F. Jaber, J.M. Chovelon, Comparative study of imazalil degradation in three systems: UV/TiO<sub>2</sub>, UV/K<sub>2</sub>S<sub>2</sub>O<sub>8</sub> and UV/TiO<sub>2</sub>/K<sub>2</sub>S<sub>2</sub>O<sub>8</sub>, *Appl. Catal., B* 144 (2014) 286–291.
- [7] Y. Wang, C.S. Hong, Effect of hydrogen peroxide, periodate and persulfate on photocatalysis of 2-chlorobiphenyl in aqueous TiO<sub>2</sub> suspensions, *Water Res.* 33 (1999) 2031–2036.
- [8] M.K. Sahoo, B. Sinha, M. Marbaniang, D.B. Naik, R.N. Sharan, Mineralization of Calcon by UV/oxidant systems and assessment of biotoxicity of the treated solutions by *E. coli* colony forming unit assay, *Chem. Eng. J.* 181–182 (2012) 206–214.
- [9] S. Yang, P. Wang, X. Yang, L. Shan, W. Zhang, X. Shao, R. Niu, Degradation efficiencies of azo dye Acid Orange 7 by the interaction of heat, UV and anions with common oxidants: Persulfate, peroxymonosulfate and hydrogen peroxide, *J. Hazard. Mater.* 179 (2010) 552–558.
- [10] M.K. Sahoo, M. Marbaniang, B. Sinha, D.B. Naik, R.N. Sharan, UVC induced TOC removal studies of Ponceau S in the presence of oxidants: Evaluation of electrical energy efficiency and assessment of biotoxicity of the treated solutions by *Escherichia coli* colony forming unit assay, *Chem. Eng. J.* 213 (2012) 142–149.
- [11] K. Selvam, M. Muruganandham, I. Muthuvel, M. Swaminathan, The influence of inorganic oxidants and metal ions on semiconductor sensitized photodegradation of 4-fluorophenol, *Chem. Eng. J.* 128 (2007) 51–57.
- [12] S. Irmak, E. Kusvuran, O. Erbatur, Degradation of 4-chloro-2-methylphenol in aqueous solution by UV irradiation in the presence of titanium dioxide, *Appl. Catal., B* 54 (2004) 85–91.
- [13] L. Ravichandran, K. Selvam, M. Swaminathan, Effect of oxidants and metal ions on photodefluorination of pentafluorobenzoic acid with ZnO, *Sep. Purif. Technol.* 56 (2007) 192–198.
- [14] C.H. Yu, C.H. Wu, T.H. Ho, P.K.A. Hong, Decolorization of C.I. Reactive Black 5 in UV/TiO<sub>2</sub>, UV/oxidant and UV/TiO<sub>2</sub>/oxidant systems: A comparative study, *Chem. Eng. J.* 158 (2010) 578–583.
- [15] N.S. Shah, X. He, H.M. Khan, J.A. Khan, K.E. Oshea, D.L. Boccelli, D.D. Dionysiou, Efficient removal of endosulfan from aqueous solution by UV-C/peroxides: A comparative study, *J. Hazard. Mater.* 263 (2013) 584–592.
- [16] C. Tan, N. Gao, Y. Deng, Y. Zhang, M. Sui, J. Deng, S. Zhou, Degradation of antipyrine by UV, UV/H<sub>2</sub>O<sub>2</sub> and UV/PS, *J. Hazard. Mater.* 260 (2013) 1008–1016.
- [17] S.Y. Yang, P. Wang, X. Yang, L. Shan, W.Y. Zhang, X.T. Shao, R. Niu, Degradation efficiencies of azo dye Acid Orange 7 by the interaction of heat, UV and anions with common oxidants: Persulfate, peroxymonosulfate and hydrogen peroxide, *J. Hazard. Mater.* 179 (2010) 552–558.
- [18] E. Hayon, A. Treinin, J. Wilf, Electronic spectra, photochemistry, and autoxidation mechanism of the sulfite–bisulfite–pyrosulfite systems. SO<sub>2</sub><sup>-</sup>, SO<sub>3</sub><sup>-</sup>, SO<sub>4</sub><sup>-</sup>, and SO<sub>5</sub><sup>-</sup> radicals, *J. Am. Chem. Soc.* 94 (1972) 47–57.
- [19] T.K. Lau, W. Chu, N.J.D. Graham, The aqueous degradation of butylated hydroxyanisole by UV/S<sub>2</sub>O<sub>8</sub><sup>2-</sup>: Study of reaction mechanisms via dimerization and mineralization, *Environ. Sci. Technol.* 41 (2007) 613–619.
- [20] D. Salari, A. Niaei, S. Aber, M.H. Rasoulifard, The photooxidative destruction of C.I. Basic Yellow 2 using UV/S<sub>2</sub>O<sub>8</sub><sup>2-</sup> process in a rectangular continuous photoreactor, *J. Hazard. Mater.* 166 (2009) 61–66.
- [21] J.L. Stauber, Toxicity of chlorate to marine microalgae, *Aquat. Toxicol.* 41 (1998) 213–227.
- [22] Z. Zuo, Y. Katsumura, Formation of hydrated electron and BrO<sub>3</sub> radical from laser photolysis of BrO<sub>3</sub><sup>-</sup> aqueous solution, *J. Chem. Soc., Faraday Trans.* 94 (1998) 3577–3580.
- [23] J.N. Sahu, J. Acharya, B.C. Meikap, Response surface modeling and optimization of chromium (VI) removal from aqueous solution using Tamarind wood activated carbon in batch process, *J. Hazard. Mater.* 172 (2009) 818–825.
- [24] C.J. Silva, I.C. Roberto, Optimization of xylitol production by *Candida guilliermondii* FTI-20037 using response surface methodology, *Process Biochem.* 36 (2001) 1119–1124.
- [25] A. Kesraoui-Abdessalem, N. Oturan, N. Bellakhal, M. Dachraoui, M.A. Oturan, Experimental design methodology applied to electro-Fenton treatment for degradation of herbicide chlortoluron, *Appl. Catal., B* 78 (2008) 334–341.
- [26] D.P. Haaland, *Experimental Design in Biotechnology*, Marcel Dekker, New York, NY, 1989.
- [27] H.L. Liu, Y.R. Chiou, Optimal decolorization efficiency of Reactive Red 239 by UV/TiO<sub>2</sub> photocatalytic process coupled with response surface methodology, *Chem. Eng. J.* 112 (2005) 173–179.

- [28] F. Francis, A. Sabu, K.M. Nampoothiri, S. Ramachandran, S. Ghosh, G. Szakacs, A. Pandey, Use of response surface methodology for optimizing process parameters for the production of  $\alpha$ -amylase by *Aspergillus oryzae*, *Biochem. Engin. J.* 15 (2003) 107–115.
- [29] G.P. Anipsitakis, D.D. Dionysiou, Transition metal/UV-based advanced oxidation technologies for water decontamination, *Appl. Catal., B* 54 (2004) 155–163.
- [30] G.P. Anipsitakis, D.D. Dionysiou, M.A. Gonzalez, Cobalt-mediated activation of peroxymonosulfate and sulfate radical attack on phenolic compounds: Implications of chloride ions, *Environ. Sci. Technol.* 40 (2006) 1000–1007.
- [31] Y.H. Guan, J. Ma, X.C. Li, J.Y. Fang, L.W. Chen, Influence of pH on the formation of sulfate and hydroxyl radicals in the UV/peroxymonosulfate system, *Environ. Sci. Technol.* 45 (2011) 9308–9314.
- [32] A.R. Khataee, O. Mirzajani, UV/peroxydisulfate oxidation of C. I. Basic Blue 3: Modeling of key factors by artificial neural network, *Desalination* 251 (2010) 64–69.
- [33] C.J. Liang, C.J. Bruell, M.C. Marley, K.L. Sperry, Thermally activated persulfate oxidation of trichloroethylene (TCE) and 1,1,1-trichloroethane (TCA) in aqueous systems and soil slurries, *Soil Sediment Contam.* 12 (2003) 207–228.
- [34] G.P. Anipsitakis, D.D. Dionysiou, Radical generation by the interaction of transition metals with common oxidants, *Environ. Sci. Technol.* 38 (2004) 3705–3712.
- [35] J. Saien, A.R. Soleymani, J.H. Sun, Parametric optimization of individual and hybridized AOPs of  $\text{Fe}^{2+}/\text{H}_2\text{O}_2$  and UV/ $\text{S}_2\text{O}_8^{2-}$  for rapid dye destruction in aqueous media, *Desalination* 279 (2011) 298–305.
- [36] P. Neta, R.E. Huie, A.B. Ross, Rate constants for reactions of inorganic radicals in aqueous solution, *J. Phys. Chem. Ref. Data* 17 (1988) 1027–1284.
- [37] M.H. Rasoulifard, H. Majidzadeh, F. Torkian Demneh, El. Babaei, M.H. Rasoulifard, Photocatalytic degradation of tylosin via ultraviolet-activated persulfate in aqueous solution, *Int. J. Ind. Chem.* 3 (2012) 1–5.
- [38] B. Rezaei, Spectrofluorimetric flow injection determination of glycerol & ethylene glycol with Alizarin Navy Blue, *Anal. Lett.* 33 (2000) 941–951.
- [39] M.S. Seyed-Dorraji, N. Daneshvar, S. Aber, Influence of inorganic oxidants and metal ions on photocatalytic activity of prepared zinc oxide nanocrystals, *Global Nest J.* 11 (2009) 535–545.
- [40] C. Lee, J. Yoon, Application of photoactivated periodate to the decolorization of reactive dye: Reaction parameters and mechanism, *J. Photochem. Photobiol., A* 165 (2004) 35–41.
- [41] W.A. Sadik, Effect of inorganic oxidants in photodecolorization of an azo dye, *J. Photochem. Photobiol., A* 191 (2007) 132–137.
- [42] N.M. Mahmoodi, M. Arami, J. Zhang, Preparation and photocatalytic activity of immobilized composite photocatalyst (titania nanoparticle/activated carbon), *J. Alloys Compd.* 509 (2011) 4754–4764.
- [43] D. Georgiou, P. Melidis, A. Aivasidis, K. Gimouhopoulos, Degradation of azo-reactive dyes by ultraviolet radiation in the presence of hydrogen peroxide, *Dyes Pigm.* 52 (2002) 69–78.